Geodesic Chaos in Stationary Spacetimes:

Numerical Study of Test-Particle Motion in a Black Hole Metric Perturbed by a Rotating Thin Disc

Claudia Caputo

claudia.caputo@matfyz.cuni.cz,

Charles University
Institute of Theoretical Physics

NEB-21
Corfu September 1-4, 2025

matfyz

Motivation

Black Hole accretion system: understanding the motion of test particles using simplified models via numerical simulations which account only for the gravitational fields and adding gradually features that make the model “as astrophysical” as possible.

Motivation

Black Hole accretion system: understanding the motion of test particles using simplified models via numerical simulations which account only for the gravitational fields and adding gradually features that make the model "as astrophysical" as possible.

Assumptions

1. Stationary, axisymmetric spacetime: Schwarzschild black hole plus a finite thin disc;
2. Disc matter follows circular orbits (circular spacetimes);
3. Keplerian condition on test-particles motion.

Metric

$$ds^2 = -e^{2\nu(r,\theta)}dt^2 + B(r,\theta)^2 r^2 e^{-2\nu(r,\theta)} \sin^2\theta(d\phi - \omega(r,\theta)dt)^2 + e^{[2\lambda(r,\theta)-2\nu(r,\theta)]}(dr^2 + r^2 d\theta^2)$$

Remarks

- **Weyl coordinate** $\rho = r\sin\theta, \quad z = r\cos\theta$
- ν, λ, ω, B to be determined by Einstein field equations

B: $$B_{,\rho\rho} + \frac{2B_\rho}{\rho} + B_{,zz} = 8\pi B(T_{\rho\rho} + T_{zz})$$

vacuum : $$T_{\mu\nu} = 0 \quad \begin{cases} B = 1 \\ B = 1 - \frac{M^2}{4(\rho^2+z^2)} = 1 - \frac{M^2}{4r^2} \end{cases} \Rightarrow \textbf{horizon} \begin{cases} \rho = 0, \quad |z| \leq M \\ r = \frac{M}{2} \end{cases}$$

- After applying adequate boundary conditions at infinity, on the axis and at the horizon, the remaining non-liner coupled equations must be solved for ν and ω and finally λ is obtained by line integration.
- Analytically solution only for static case $\omega = 0$
- Non static case:
  1. generating technique
  2. perturbative approach ✓ Will,1974

Semerák, O.; Čížek, P. Rotating Disc around a Schwarzschild Black Hole. Universe 2020, 6, 27.
P. Čížek and O. Semerák 2017 ApJS 232 14

How does the disk's rotation, that is the "frame-dragging", influence the chaotic dynamics of geodesics?

How does the disk's rotation, that is the "frame-dragging", influence the chaotic dynamics of geodesics?

Overall picture from previous literature

- The frame dragging induced by rotation of the system seems to lead to a suppression of the chaotic behaviour **?**;
- The counter-rotating motion appears to be more unstable than the co-rotating motion

- **Chaos and rotating black holes with halos**
  P.S. Letelier (Campinas State U., IMECC), W.M. Vieira (Campinas State U., IMECC), Phys.Rev.D 56 (1997), 8095-8098
- **Stability of Orbits around a Spinning Body in a Pseudo-Newtonian Hill Problem**
  A.F. Steklain (Campinas State U., IMECC), P.S. Letelier (Campinas State U., IMECC), Phys.Lett.A 373 (2009), 188-194.
- **Influence of the black hole spin on the chaotic particle dynamics within a dipolar halo** Sankhasubhra Nag, Siddhartha Sinha, Deepika B. Ananda, Tapas K Das, Astrophys.Space Sci. 362 (2017) 4, 81.
- **Stealth Chaos due to Frame Dragging** Andrés F. Gutiérrez-Ruiz, Alejandro Cárdenas-Avendaño, Nicolás Yunes, Leonardo A. Pachón,abff99

Physical interpretation & Keplerian-compatible parameters

Physical interpretation of the disc

Two standard representations:

- **One–component perfect fluid**: specified by surface density, azimuthal pressure, and circular velocity;
- **Two–stream dust**: two counter–rotating geodesic streams on the disc with surface densities $\sigma_\pm$ and velocities $v_\pm$ in the stationary limit. Physical admissibility requires $\sigma_\pm \geq 0$.

Physical interpretation & Keplerian-compatible parameters

Physical interpretation of the disc

Two standard representations:

- **One–component perfect fluid**: specified by surface density, azimuthal pressure, and circular velocity;
- **Two–stream dust**: two counter–rotating geodesic streams on the disc with surface densities $\sigma_\pm$ and velocities $v_\pm$ in the stationary limit. Physical admissibility requires $\sigma_\pm \geq 0$.

Keplerian regime on parameter's space

$$\sigma_-\left(\frac{x_{in}+x_{out}}{2}\right)=0, \qquad S=k(x_*)\,W.$$

1. **Astrophysical meaning:** retrograde stream extinguished, prograde circular flow retained; rotation consistent with Keplerian scaling $\Omega \propto r^{-3/2}$ at large radii.
2. **Stream balance:** minimises counter–rotating stream imbalance, reducing derivative jumps of the metric across the disc plane.
3. **Parameter-space boundary:** separates the admissible region $S \geq k(x_*)W$ from the unphysical one $S < k(x_*)W$.

Investigating dragging effect

- **Physical System**: Schwarzschild Black Hole + Rotating Thin Disk (Will-Semerák-Ĉiẑek solution).
- The disk introduces non-integrable perturbations to the spacetime metric.
- **Primary Chaos Source**: Metric discontinuities at the sharp disk edges act as sites for impulsive scattering.
- **Open Question**: How does the disk's rotation (frame-dragging) influence the chaotic dynamics of geodesics?

The Dragging Parameter W

$W > 0$: Co-rotating (R)
$W < 0$: Counter-rotating (CR)
$W = 0$: Static (S) case

Methods for detecting choas

Poincaré surface of section

Let H be a Hamiltonian autonomous system with $2n$ degrees of freedom. Since the energy is conserved, the phase space can be reduced to $2n-1$-surfaces.
A surface of section is then obtained by

1. $q_i = const$, set another degree of freedom as constant
2. take the value of the other $2n-2$ degrees of freedom $(p_1, \ldots, p_{(n-2)}, q_1, \ldots, q_{(n-2)})$, each time the orbits cross the hyper surface defined by $q_i = const$ (in a fixed direction)

Poincaré surface of section

Let H be a Hamiltonian autonomous system with $2n$ degrees of freedom. Since the energy is conserved, the phase space can be reduced to $2n-1$-surfaces.
A surface of section is then obtained by

1. $q_i = const$, set another degree of freedom as constant
2. take the value of the other $2n-2$ degrees of freedom $(p_1, \ldots, p_{(n-2)}, q_1, \ldots, q_{(n-2)})$, each time the orbits cross the hyper surface defined by $q_i = const$ (in a fixed direction)

Remarks

- **Resonant tori**: manifest itself as infinite set of points;
- **Non- resonant tori**: appear as a succession of points which cover densely the invariant curves.
  PS give an overall view of the dynamics of the system and of the accessible states of the system

Local vs Global Indicators in Frame-Dragging Settings

Limitations of Local Approaches

- Sensitive to initial conditions
- Provide limited information about phase space structure
- Difficult to characterize "stickiness" and weak chaos
- Cannot quantify overall system chaoticity

Local vs Global Indicators in Frame-Dragging Settings

Limitations of Local Approaches

- Sensitive to initial conditions
- Provide limited information about phase space structure
- Difficult to characterize "stickiness" and weak chaos
- Cannot quantify overall system chaoticity

The Dragging Effect Challenge

- Need methods that capture global chaotic properties
- Requires statistical approach beyond individual trajectories

Local vs Global Indicators in Frame-Dragging Settings

Limitations of Local Approaches

- Sensitive to initial conditions
- Provide limited information about phase space structure
- Difficult to characterize "stickiness" and weak chaos
- Cannot quantify overall system chaoticity

The Dragging Effect Challenge

- Need methods that capture global chaotic properties
- Requires statistical approach beyond individual trajectories

Strategy: Combine local indicators (instantaneous stretching) with a global indicator(phase-space information production):

1. Local: Lyapunov exponents; fast diagnostics FLI and MEGNO.
2. Global: Kolmogorov–Sinai (KS) entropy to aggregate over the invariant measure.

Lyapunov Exponents: Local Chaos Measure

Definition

Maximum Lyapunov Exponent (mLE) quantifies exponential divergence of nearby trajectories:

$$\lambda_{\text{max}} = \lim_{t\to\infty} \frac{1}{t} \ln \frac{\|\delta x(t)\|}{\|\delta x(0)\|}, \quad \dot{\delta x} = Df(x(t))\,\delta x$$

- $\lambda > 0$: Chaotic orbit (exponential divergence)
- $\lambda = 0$: Regular orbit (polynomial divergence)
- $\lambda < 0$: Stable fixed point (convergence)

Local method: Characterizes behaviour in specific phase space regions.

Numerical estimation: Computed via the Benettin (Gram–Schmidt) algorithm; finite-time estimates diagnose localized instability and stickiness[1].

[1] Benettin et al. (1980) - Lyapunov exponents computation

Fast Diagnostics: FLI and MEGNO (Definitions)

Definition:Fast Lyapunov Indicator (FLI)

$$\mathrm{FLI}(t) \; = \; \ln \frac{\|\xi(t)\|}{\|\xi(0)\|}$$

1. Chaotic orbits: $\mathrm{FLI}(t) \sim \lambda t$;
2. Regular orbit: sub-linear/polynomial growth

Fast Diagnostics: FLI and MEGNO (Definitions)

Definition: Fast Lyapunov Indicator (FLI)

$$\mathrm{FLI}(t) \;=\; \ln\frac{\|\xi(t)\|}{\|\xi(0)\|}$$

1. Chaotic orbits: $\mathrm{FLI}(t) \sim \lambda t$;
2. Regular orbit: sub-linear/polynomial growth

Definition: Mean Exponential Growth of Nearby Orbits (MEGNO)

$$Y(t) \;=\; \frac{2}{t}\int_0^t \frac{d}{ds}\big(\ln\|\xi(s)\|\big)\, s\, ds$$

1. Chaotic orbits: $Y(t) \sim \lambda t$ (slope $\approx \lambda$).
2. Regular orbit: $Y(t) \to 2$.

Advantages: Rapid discrimination (pre-asymptotic), complementary to rigorous Lyapunov estimates.

Froeschlé et al. (1997) - FLI definition and applications.
Cincotta & Simó (2000) - MEGNO method.

Kolmogorov-Sinai Entropy: Global Chaos Measure

Definition:Kolmogorov-Sinai Entropy

Measures the rate of information production in dynamical systems:

$$h_{KS} = \sup_{\mathcal{P}} \lim_{t\to\infty} \frac{1}{t} H(\mathcal{P}^t)$$

- Quantifies overall unpredictability of the system
- Related to Lyapunov exponents through Pesin's formula:

$$h_{KS} = \int_M \sum_{\lambda_i(x)>0} \lambda_i(x)\, d\mu(x)$$

Global method: Integrates over the entire phase space.

Pesin (1977) - Entropy-formula connection.

Numerical Estimation of KS Entropy

- Direct method: Partition phase space and track trajectory visits
- Lyapunov-based method: Sum of positive Lyapunov exponents
- Return-time statistics: Analyse distribution of recurrence times
- Poincaré section approach: Measure complexity on reduced phase space

Practical Implementation

$$h_{KS} \approx \frac{\sum T_i \lambda_i}{\sum T_i}$$

Time-weighted average of local Lyapunov exponents along trajectories

Numerical Methodology summary

Qualitative Tool

- **Poincaré Surfaces of Section (PSS)**
- Plot crossing points in phase space.
- Colored by the MEGNO chaos indicator.
- Reveals structure: KAM tori vs. chaotic seas.

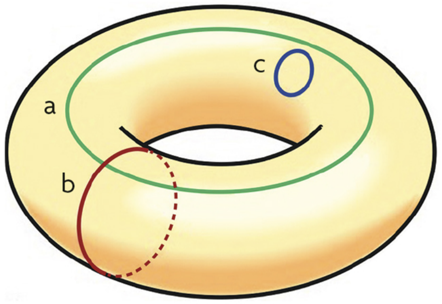

Quantitative Tool

- **Kolmogorov-Sinai Entropy (h_{KS})**
- Measures the global rate of chaos production.
- Calculated as:

$$h_{KS} = \theta \cdot \bar{\lambda}$$

- θ: Fraction of chaotic orbits.
- $\bar{\lambda}$: Mean Lyapunov exponent of chaotic orbits.

The Four Dynamical Cases Investigated

Case	Orbital domain	Disk crossings?	Primary mechanism

The Four Dynamical Cases Investigated

Case	Orbital domain	Disk crossings?	Primary mechanism
1	$r > r_{\text{Sch}},\ r_{\text{in}} = 7M$	✓	Edge scattering at disk boundaries

The Four Dynamical Cases Investigated

Case	Orbital domain	Disk crossings?	Primary mechanism
1	$r > r_{\mathrm{Sch}},\ r_{\mathrm{in}} = 7M$	✓	Edge scattering at disk boundaries
2	$r > r_{\mathrm{Sch}},\ r_{\mathrm{in}} = 18M,\ r_{\mathrm{out}} = 22M$	✓	Scattering + effective-potential modulation

The Four Dynamical Cases Investigated

Case	Orbital domain	Disk crossings?	Primary mechanism
1	$r > r_{\mathrm{Sch}},\ r_{\mathrm{in}} = 7M$	✓	Edge scattering at disk boundaries
2	$r > r_{\mathrm{Sch}},\ r_{\mathrm{in}} = 18M,\ r_{\mathrm{out}} = 22M$	✓	Scattering + effective-potential modulation
3	$r_{\mathrm{Sch}} < r < r_{\mathrm{in}} = 16M$	✗	None (integrable baseline)

The Four Dynamical Cases Investigated

Case	Orbital domain	Disk crossings?	Primary mechanism
1	$r > r_{\rm Sch},\ r_{\rm in} = 7M$	✓	Edge scattering at disk boundaries
2	$r > r_{\rm Sch},\ r_{\rm in} = 18M,\ r_{\rm out} = 22M$	✓	Scattering + effective-potential modulation
3	$r_{\rm Sch} < r < r_{\rm in} = 16M$	✗	None (integrable baseline)
4	$r_{\rm Sch} < r < r_{\rm in} = 29M$	✗	Weak resonance breaking

Case 1 — ($E = 0.945,\ L_z = 3.75,\ x_{\rm in} = 6,\ x_{\rm out} = 10,\ S = 4.97359 \times 10^{-4},\ M_d \approx 0.1M$)

Static → Co-rotating → Counter-rotating

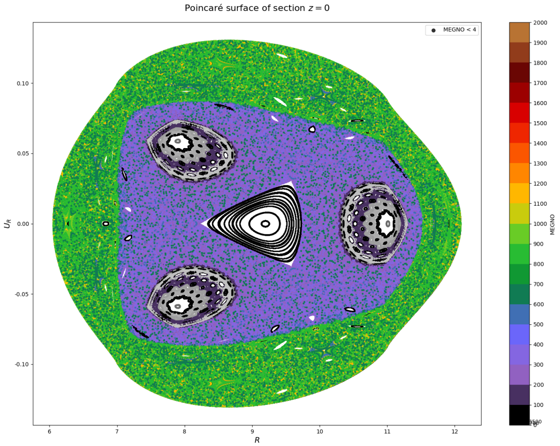

S1: $W = 0$ (static)

Case 1 — ($E = 0.945,\ L_z = 3.75,\ x_{\rm in} = 6,\ x_{\rm out} = 10,\ S = 4.97359 \times 10^{-4},\ M_d \approx 0.1M$)

Static → Co-rotating → Counter-rotating

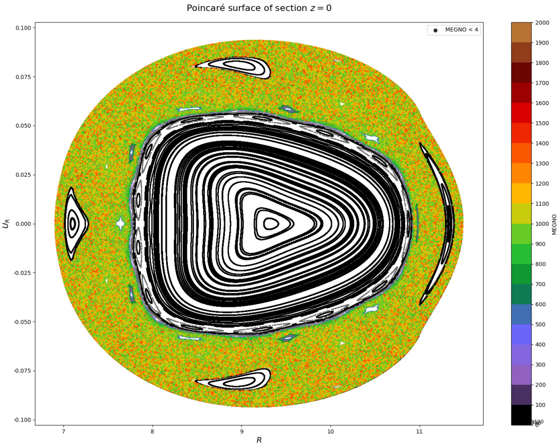

R2: $W \approx +0.5$ (sub-K)

Case 1 — ($E = 0.945$, $L_z = 3.75$, $x_{\rm in} = 6$, $x_{\rm out} = 10$, $S = 4.97359 \times 10^{-4}$, $M_d \approx 0.1M$)

Static → Co-rotating → Counter-rotating

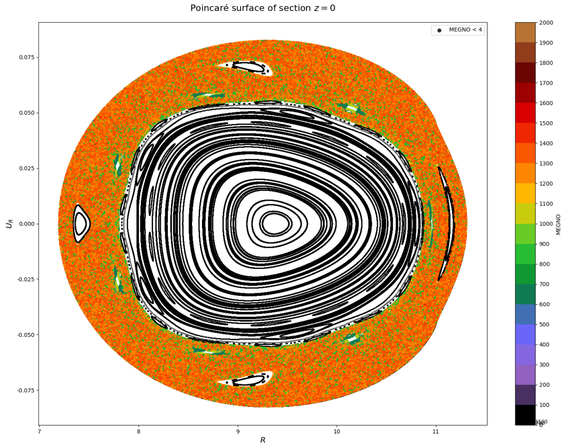

R1: $W \approx +0.6$ (Keplerian)

Case 1 — ($E = 0.945$, $L_z = 3.75$, $x_{\rm in} = 6$, $x_{\rm out} = 10$, $S = 4.97359 \times 10^{-4}$, $M_d \approx 0.1M$)

Static → Co-rotating → Counter-rotating

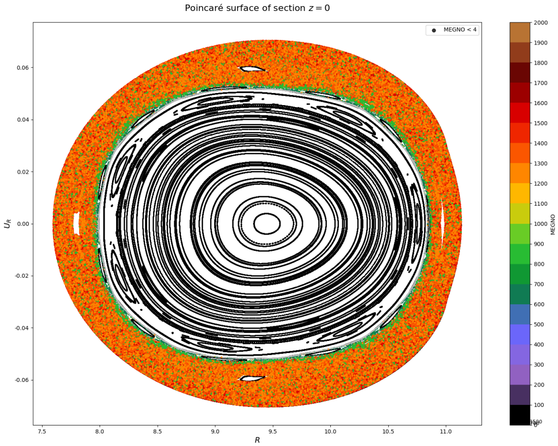

R3: $W \approx +0.8$ (super-K)

Case 1 — ($E = 0.945$, $L_z = 3.75$, $x_{\rm in} = 6$, $x_{\rm out} = 10$, $S = 4.97359 \times 10^{-4}$, $M_d \approx 0.1M$)

Static → Co-rotating → Counter-rotating

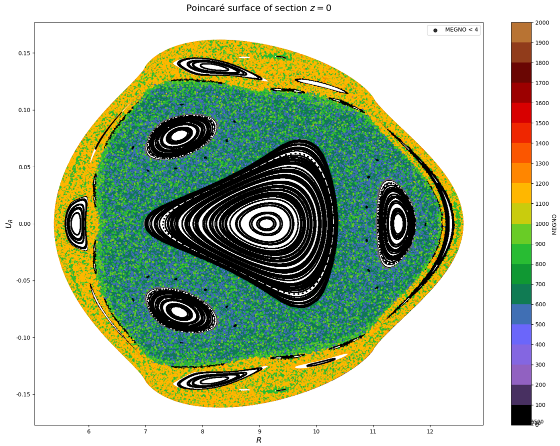

CR2: $W \approx -0.5$ (sub-K)

Case 1 — ($E = 0.945$, $L_z = 3.75$, $x_{\rm in} = 6$, $x_{\rm out} = 10$, $S = 4.97359 \times 10^{-4}$, $M_d \approx 0.1M$)

Static → Co-rotating → Counter-rotating

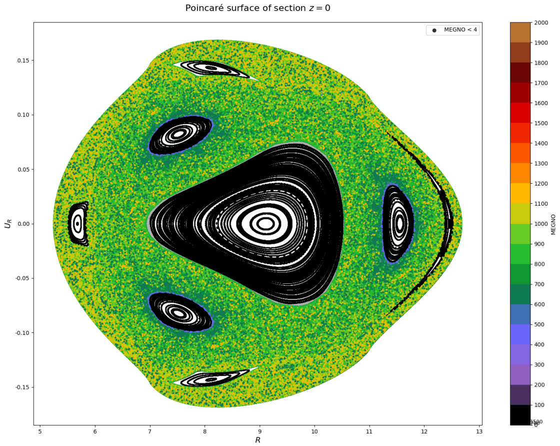

CR1: $W \approx -0.6$ (Keplerian magnitude)

Case 1 — ($E = 0.945$, $L_z = 3.75$, $x_{\rm in} = 6$, $x_{\rm out} = 10$, $S = 4.97359 \times 10^{-4}$, $M_d \approx 0.1M$)

Static → Co-rotating → Counter-rotating

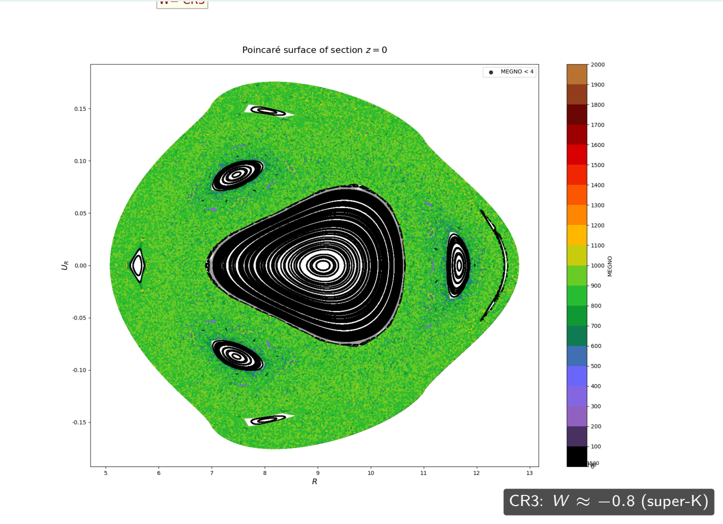

Case 2 — $(E = 0.98,\ L_z = 3.95,\ x_{\rm in} = 17,\ x_{\rm out} = 21,\ S = 2.0941 \times 10^{-5},\ M_d \approx 0.01\,M)$

Static → Co-rotating → Counter-rotating

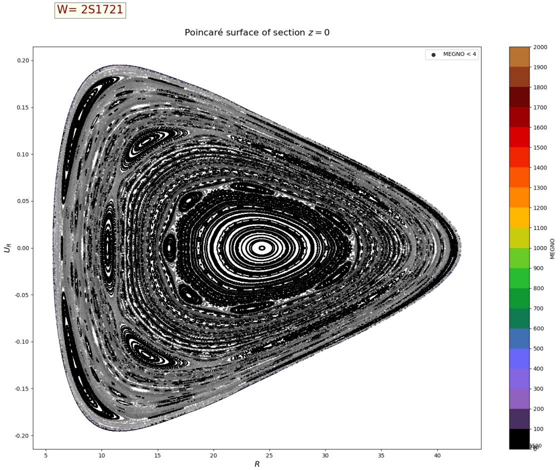

2S1721: $W = 0$ (static)

Case 2 — ($E = 0.98$, $L_z = 3.95$, $x_{\rm in} = 17$, $x_{\rm out} = 21$, $S = 2.0941 \times 10^{-5}$, $M_d \approx 0.01\,M$)

Static → Co-rotating → Counter-rotating

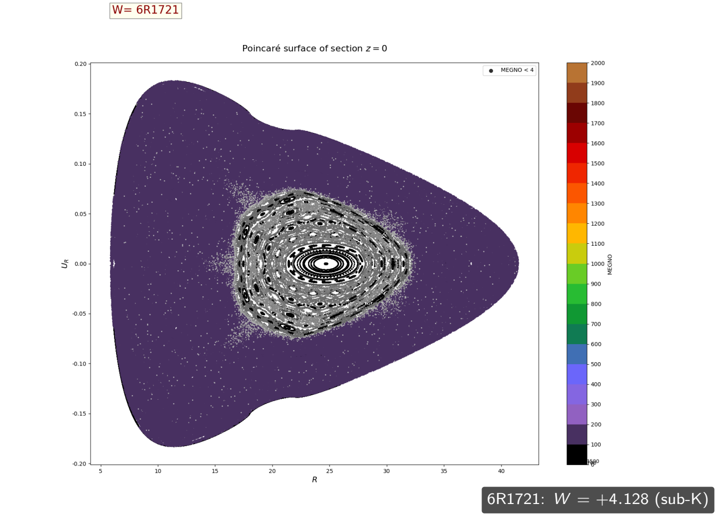

Case 2 — $(E = 0.98,\ L_z = 3.95,\ x_{\rm in} = 17,\ x_{\rm out} = 21,\ S = 2.0941 \times 10^{-5},\ M_d \approx 0.01\,M)$

Static → Co-rotating → Counter-rotating

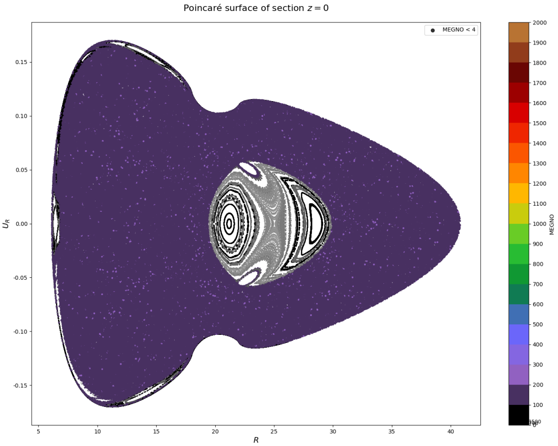

5R1721: $W = +8.256$ (sub-K)

Case 2 — $(E = 0.98,\ L_z = 3.95,\ x_{\rm in} = 17,\ x_{\rm out} = 21,\ S = 2.0941 \times 10^{-5},\ M_d \approx 0.01\ M)$

Static $\rightarrow$ Co-rotating $\rightarrow$ Counter-rotating

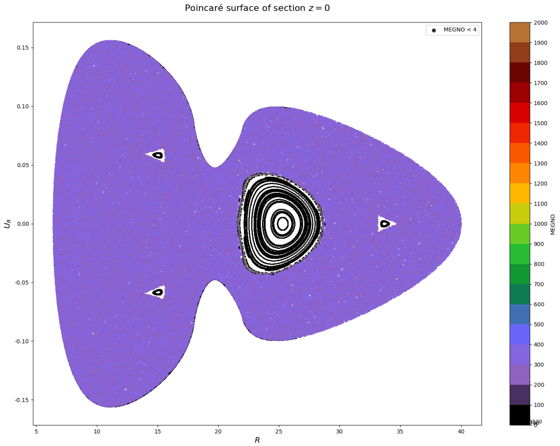

4R1721: $W = +12.384$ (sub-K)

Case 2 — ($E = 0.98$, $L_z = 3.95$, $x_{\rm in} = 17$, $x_{\rm out} = 21$, $S = 2.0941 \times 10^{-5}$, $M_d \approx 0.01\, M$)

Static → Co-rotating → Counter-rotating

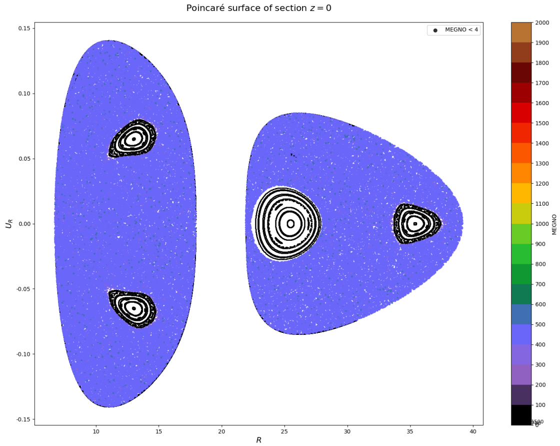

3R1721: $W = +16.512$ (sub-K)

Case 2 — $(E = 0.98,\ L_z = 3.95,\ x_{\rm in} = 17,\ x_{\rm out} = 21,\ S = 2.0941 \times 10^{-5},\ M_d \approx 0.01\, M)$

Static $\rightarrow$ Co-rotating $\rightarrow$ Counter-rotating

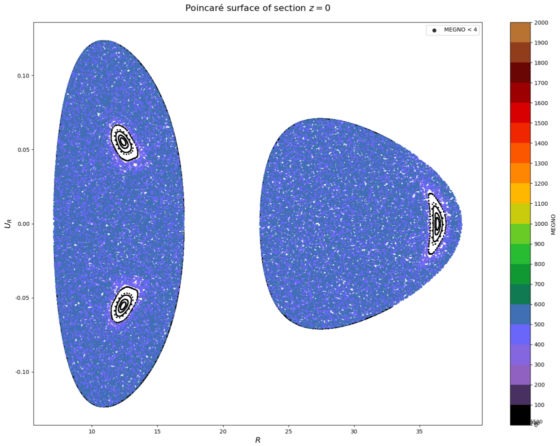

2R1721: $W = +20.640$ (Keplerian)

Case 2 — ($E = 0.98$, $L_z = 3.95$, $x_{\rm in} = 17$, $x_{\rm out} = 21$, $S = 2.0941 \times 10^{-5}$, $M_d \approx 0.01\, M$)

Static → Co-rotating → Counter-rotating

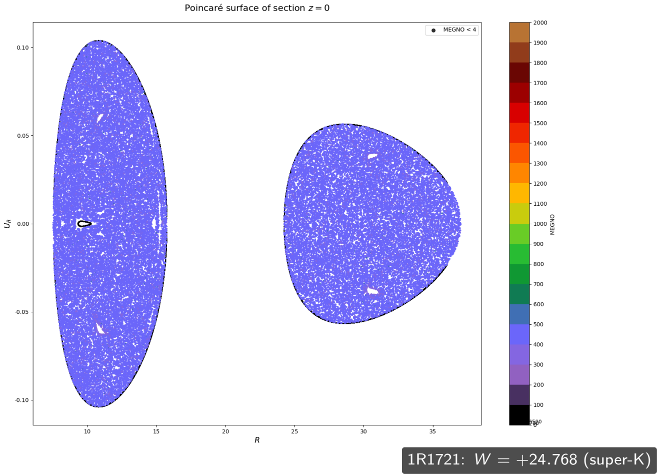

Case 2 — ($E = 0.98$, $L_z = 3.95$, $x_{\rm in} = 17$, $x_{\rm out} = 21$, $S = 2.0941 \times 10^{-5}$, $M_d \approx 0.01\,M$)

Static → Co-rotating → Counter-rotating

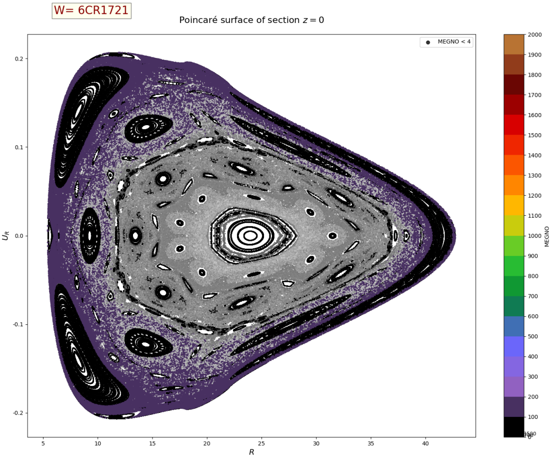

6CR1721: $W = -4.128$ (sub-K)

Case 2 — ($E = 0.98,\ L_z = 3.95,\ x_{\rm in} = 17,\ x_{\rm out} = 21,\ S = 2.0941 \times 10^{-5},\ M_d \approx 0.01\, M$)

Static → Co-rotating → Counter-rotating

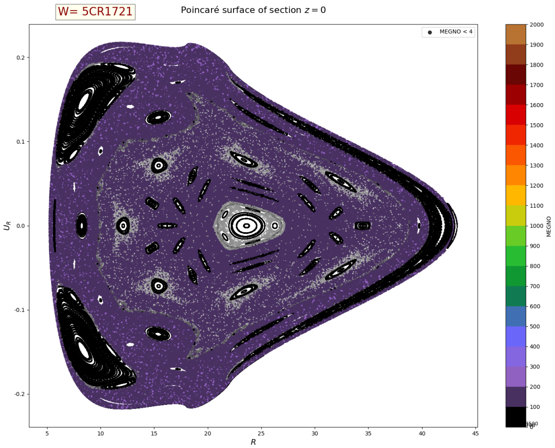

5CR1721: $W = -8.256$ (sub-K)

Case 2 — $(E = 0.98,\ L_z = 3.95,\ x_{\rm in} = 17,\ x_{\rm out} = 21,\ S = 2.0941 \times 10^{-5},\ M_d \approx 0.01\,M)$

Static → Co-rotating → Counter-rotating

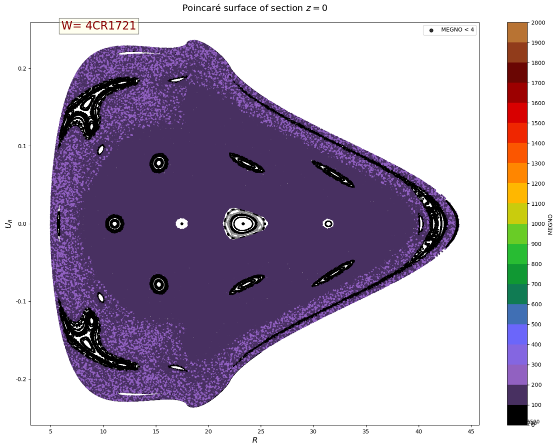

4CR1721: $W = -12.384$ (sub-K)

Case 2 — $(E = 0.98,\ L_z = 3.95,\ x_{\rm in} = 17,\ x_{\rm out} = 21,\ S = 2.0941 \times 10^{-5},\ M_d \approx 0.01\, M)$

Static $\rightarrow$ Co-rotating $\rightarrow$ Counter-rotating

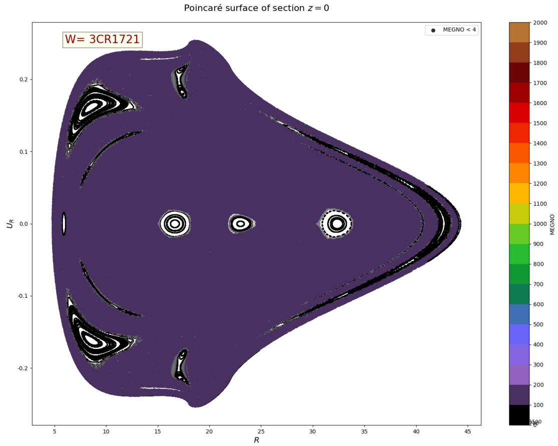

3CR1721: $W = -16.512$ (sub-K)

Case 2 — ($E = 0.98$, $L_z = 3.95$, $x_{\rm in} = 17$, $x_{\rm out} = 21$, $S = 2.0941 \times 10^{-5}$, $M_d \approx 0.01\, M$)

Static → Co-rotating → Counter-rotating

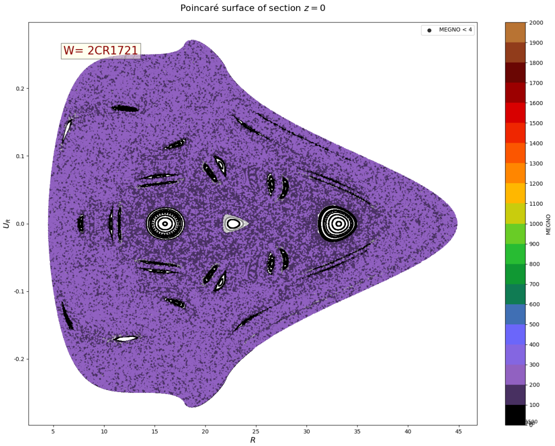

2CR1721: $W = -20.640$ (Keplerian $|W|$)

Case 2 — ($E = 0.98$, $L_z = 3.95$, $x_{\text{in}} = 17$, $x_{\text{out}} = 21$, $S = 2.0941 \times 10^{-5}$, $M_d \approx 0.01\, M$)

Static $\to$ Co-rotating $\to$ Counter-rotating

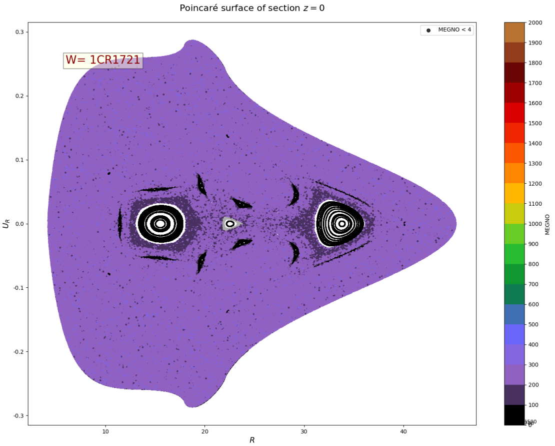

1CR1721: $W = -24.768$ (super-K)

Case 3 — ($E = 0.949$, $L_z = 3.75$, $x_{\text{in}} = 15$, $x_{\text{out}} = 18$, $S = 3.21525 \times 10^{-4}$, $M_d \approx 0.1\,M$)

Static → Co-rotating → Counter-rotating

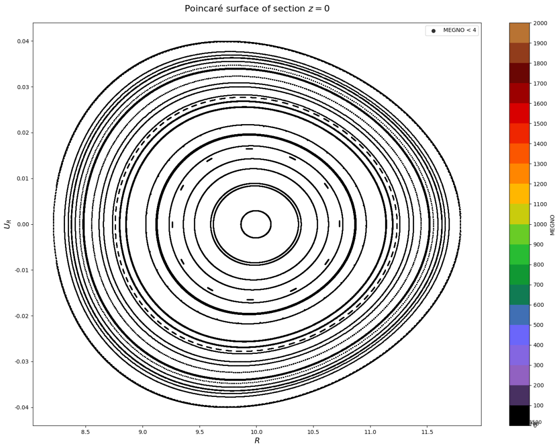

INDS1: $W = 0$ (static, all regular)

Case 3 — $(E = 0.949,\ L_z = 3.75,\ x_{\rm in} = 15,\ x_{\rm out} = 18,\ S = 3.21525 \times 10^{-4},\ M_d \approx 0.1\,M)$

Static → Co-rotating → Counter-rotating

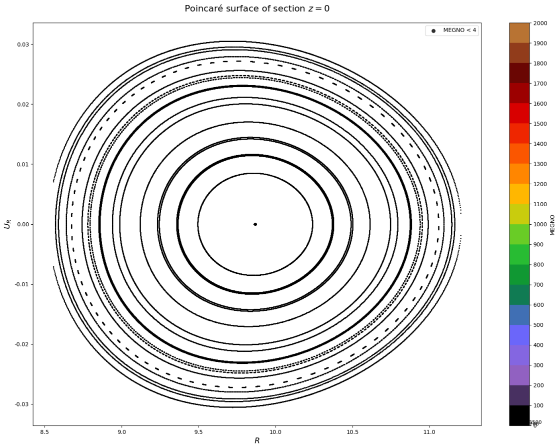

INDR0: $W = +0.591577544$ (sub-K, -50%)

Case 3 — ($E = 0.949$, $L_z = 3.75$, $x_{\rm in} = 15$, $x_{\rm out} = 18$, $S = 3.21525 \times 10^{-4}$, $M_d \approx 0.1\,M$)

Static $\rightarrow$ Co-rotating $\rightarrow$ Counter-rotating

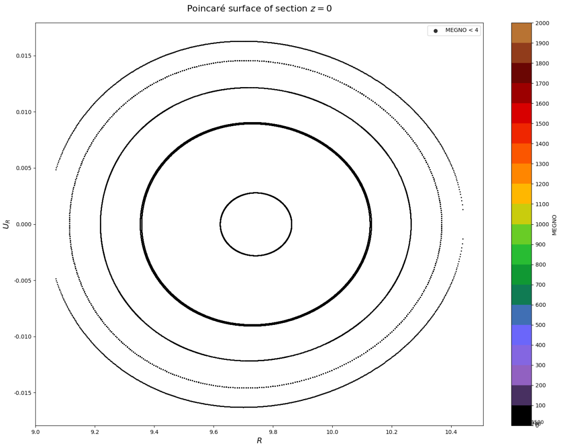

INDR1: $W = +1.183155087$ (Keplerian)

Case 3 — $(E = 0.949,\ L_z = 3.75,\ x_{\rm in} = 15,\ x_{\rm out} = 18,$ $S = 3.21525 \times 10^{-4},\ M_d \approx 0.1\,M)$

Static $\rightarrow$ Co-rotating $\rightarrow$ Counter-rotating

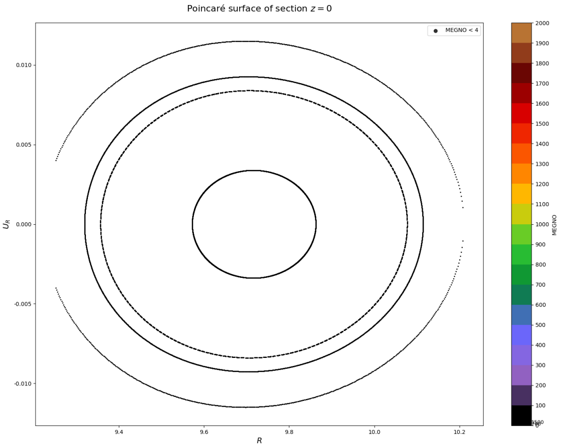

INDR10: $W = +1.301470596$ (+10%, super-K mild)

Case 3 — $(E = 0.949,\ L_z = 3.75,\ x_{\rm in} = 15,\ x_{\rm out} = 18,$ $S = 3.21525 \times 10^{-4},\ M_d \approx 0.1\,M)$

Static → Co-rotating → Counter-rotating

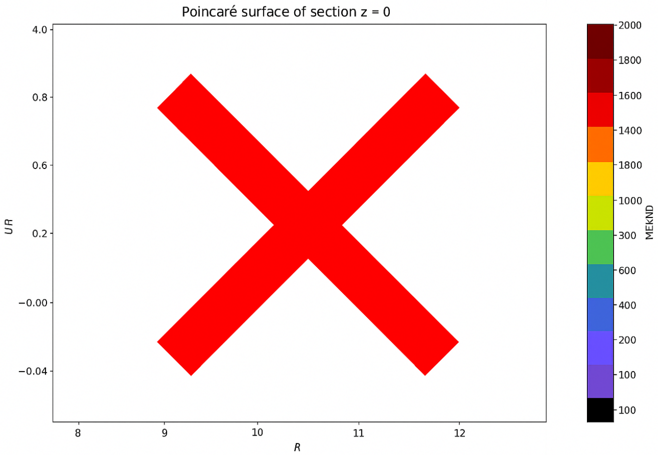

INDR2: $W = +1.774732631$ (+50%, no intersections)

Case 3 — ($E = 0.949$, $L_z = 3.75$, $x_{\rm in} = 15$, $x_{\rm out} = 18$, $S = 3.21525 \times 10^{-4}$, $M_d \approx 0.1\,M$)

Static → Co-rotating → Counter-rotating

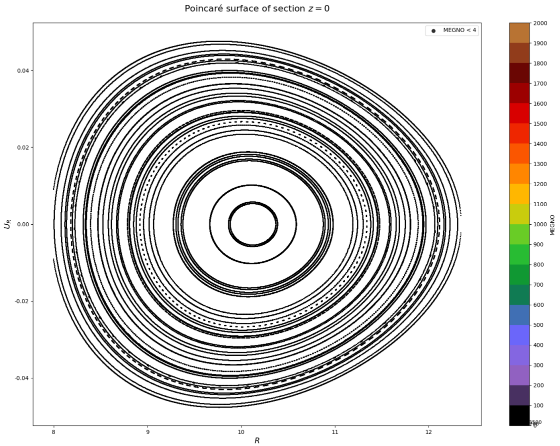

INDCR0: $W = -0.591577544$ (sub-K mag., -50%)

Case 3 — $(E = 0.949,\ L_z = 3.75,\ x_{\text{in}} = 15,\ x_{\text{out}} = 18,$ $S = 3.21525 \times 10^{-4},\ M_d \approx 0.1\,M)$

Static → Co-rotating → Counter-rotating

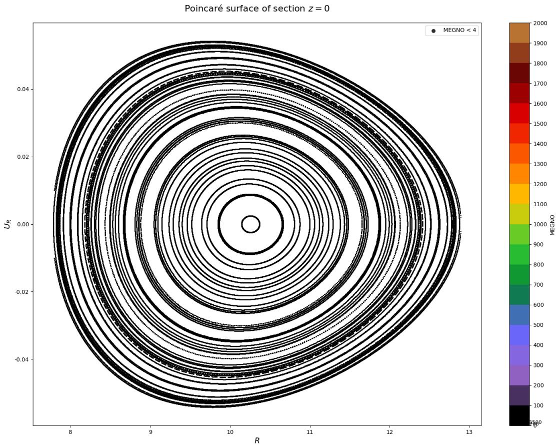

INDCR1: $W = -1.183155087$ (Keplerian $|W|$)

Case 3 — $(E = 0.949,\ L_z = 3.75,\ x_{\rm in} = 15,\ x_{\rm out} = 18,$ $S = 3.21525 \times 10^{-4},\ M_d \approx 0.1\,M)$

Static $\rightarrow$ Co-rotating $\rightarrow$ Counter-rotating

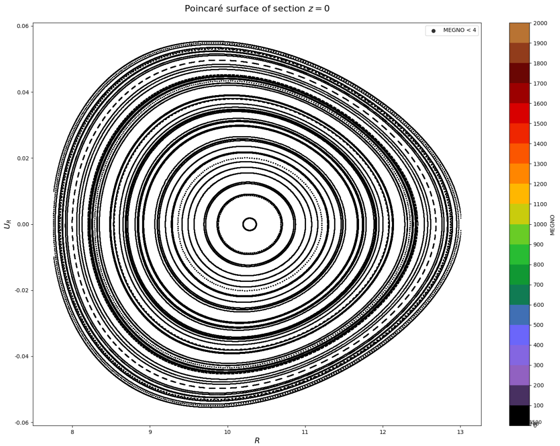

INDCR10: $W = -1.301470596$ $(+10\%\ |W|)$

Case 3 — ($E = 0.949$, $L_z = 3.75$, $x_{\rm in} = 15$, $x_{\rm out} = 18$, $S = 3.21525 \times 10^{-4}$, $M_d \approx 0.1\,M$)

Static $\rightarrow$ Co-rotating $\rightarrow$ Counter-rotating

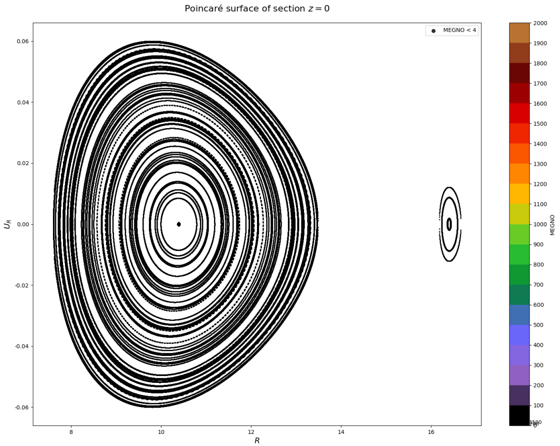

INDCR2: $W = -1.774732631$ (+50% $|W|$, fragmented regular domains)

Case 4 — ($E = 0.965$, $L_z = 3.76$, $x_{in} = 28$, $x_{out} = 30$, $S = 2.74405 \times 10^{-4}$, *disk mass* $\simeq 0.1\,M$)

Static → Co-rotating → Counter-rotating

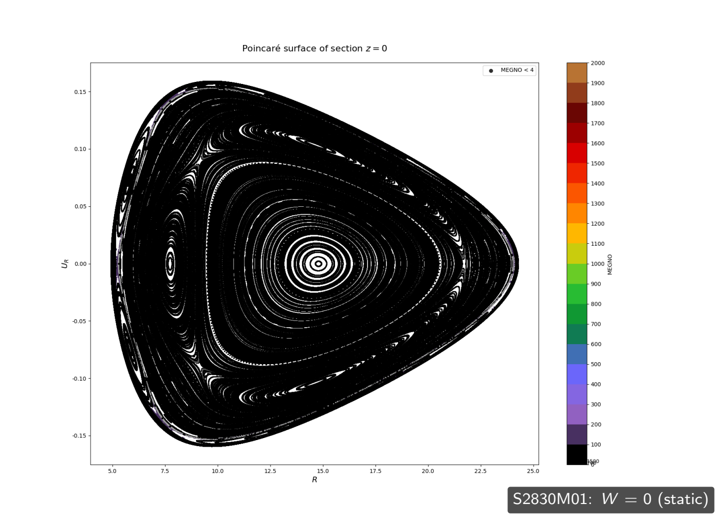

Case 4 — ($E = 0.965$, $L_z = 3.76$, $x_{in} = 28$, $x_{out} = 30$, $S = 2.74405 \times 10^{-4}$, *disk mass* $\simeq 0.1\,M$)

Static → Co-rotating → Counter-rotating

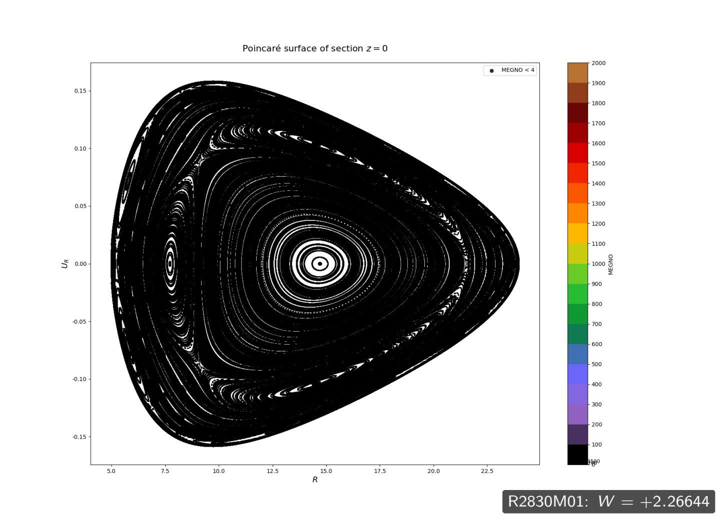

Case 4 — $(E = 0.965,\ L_z = 3.76,\ x_{in} = 28,\ x_{out} = 30, S = 2.74405 \times 10^{-4},$ $\textit{disk mass} \simeq 0.1\,M)$

Static → Co-rotating → Counter-rotating

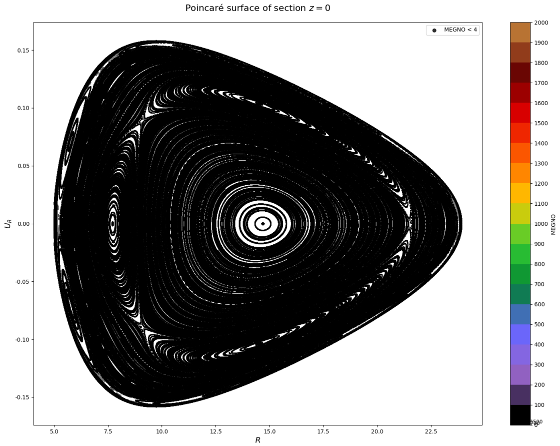

R22830M01: $W = +2.719728$

Case 4 — ($E = 0.965$, $L_z = 3.76$, $x_{in} = 28$, $x_{out} = 30$, $S = 2.74405 \times 10^{-4}$, *disk mass* $\simeq 0.1\,M$)

Static → Co-rotating → Counter-rotating

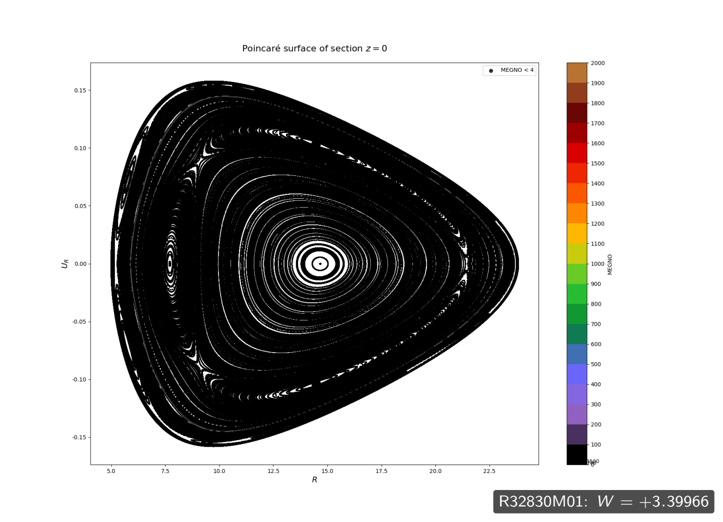

Case 4 — $(E = 0.965,\ L_z = 3.76,\ x_{in} = 28,\ x_{out} = 30, S = 2.74405 \times 10^{-4},$ $disk\ mass \simeq 0.1\ M)$

Static → Co-rotating → Counter-rotating

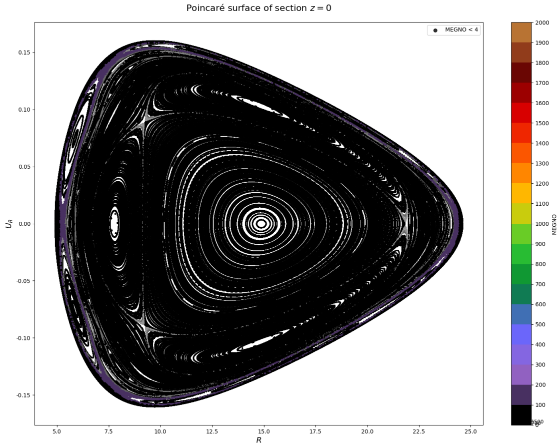

CR2830M01: $W = -2.26644$

Case 4 — ($E = 0.965$, $L_z = 3.76$, $x_{in} = 28$, $x_{out} = 30$, $S = 2.74405 \times 10^{-4}$, *disk mass* $\simeq 0.1\,M$)

Static $\rightarrow$ Co-rotating $\rightarrow$ Counter-rotating

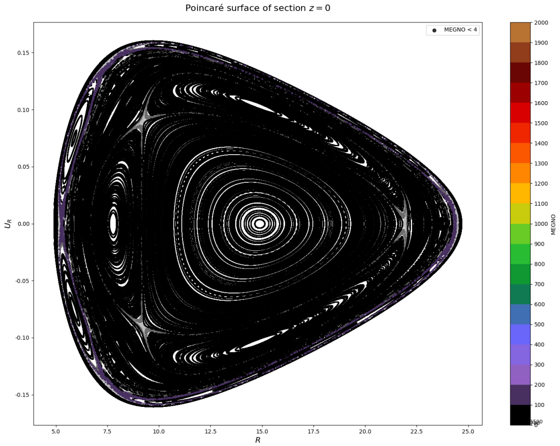

CR22830M01: $W = -2.719728$

Case 4 — $(E = 0.965,\ L_z = 3.76,\ x_{in} = 28,\ x_{out} = 30, S = 2.74405 \times 10^{-4},$ $disk\ mass \simeq 0.1\ M)$

Static → Co-rotating → Counter-rotating

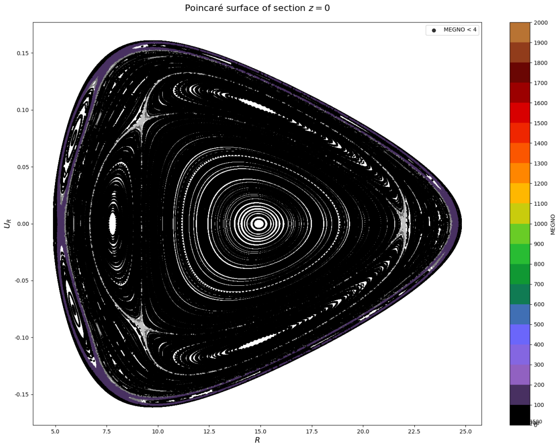

CR32830M01: $W = -3.39966$

Quantitative synthesis: global chaos trends via KS-entropy

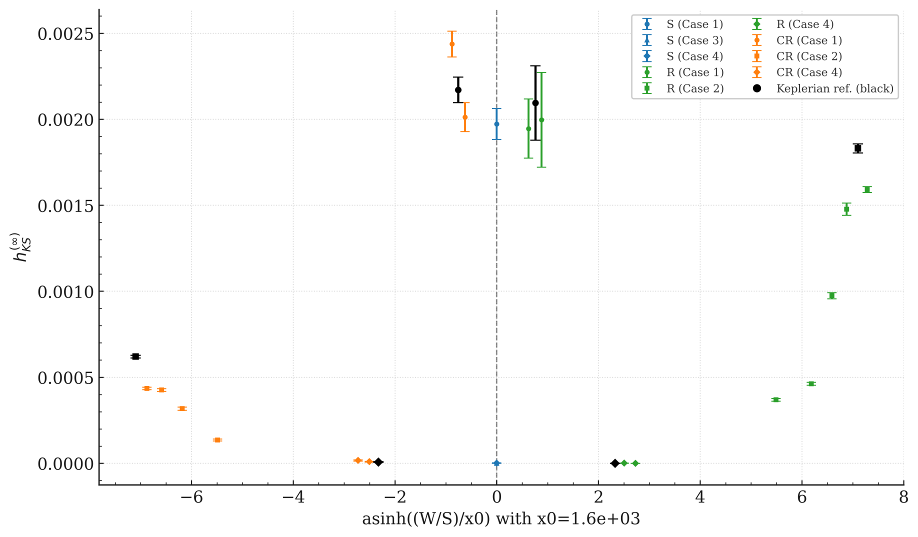

Conclusions

Synthesis: key observations and qualified evidence

1. **Case 1:** $h_{KS} \sim 10^{-3}$; **strong chaos** dominated by edge scattering; CR $>$ R.
Qualification: strength and morphology are modulated by W and its direction.
2. **Case 2:** $h_{KS} \sim 10^{-4} - 10^{-3}$; disruptive chaos with pronounced asymmetry; R $\gg$ CR.
Qualification: again controlled by W and rotation sense.
3. **Case 3:** $h_{KS} = 0$ in our sets: the disk perturbation is too small compared with Schwarzschild for the chosen $(E, L_z, S, \text{radii})$.
Qualification: this is **not** a general rule "no crossings $\Rightarrow$ no chaos".
4. **Case 4:** $h_{KS} \sim 10^{-6} - 10^{-5}$; **weak chaos without crossings**, most evident in counter-rotation and increasing with $|W|$.
Qualification: a thin chaotic layer (MEGNO $\gtrsim 100$) appears when the disk potential and frame dragging are non-negligible.

Conclusions

Synthesis: key observations and qualified evidence

1. **Case 1:** $h_{KS} \sim 10^{-3}$; **strong chaos** dominated by edge scattering; CR $>$ R.
   Qualification: strength and morphology are modulated by W and its direction.
2. **Case 2:** $h_{KS} \sim 10^{-4} - 10^{-3}$; disruptive chaos with pronounced asymmetry; R $\gg$ CR.
   Qualification: again controlled by W and rotation sense.
3. **Case 3:** $h_{KS} = 0$ in our sets: the disk perturbation is too small compared with Schwarzschild for the chosen $(E, L_z, S, \text{radii})$.
   Qualification: this is **not** a general rule "no crossings $\Rightarrow$ no chaos".
4. **Case 4:** $h_{KS} \sim 10^{-6} - 10^{-5}$; **weak chaos without crossings**, most evident in counter-rotation and increasing with $|W|$.
   Qualification: a thin chaotic layer (MEGNO $\gtrsim 100$) appears when the disk potential and frame dragging are non-negligible.

Main Message

Chaotic dynamics is primarily driven by scattering at the sharp disk edges.
Frame dragging W is a **secondary control parameter** that enhances or suppresses chaos depending on the orbital domain and the rotation sense (R vs. CR).


Thanks for listening
I am done.
Goodbye!

References

1. Semerák, O.; Čížek, P. Rotating Disc around a Schwarzschild Black Hole. Universe 2020, 6, 27.
2. P. Čížek and O. Semerák 2017 ApJS 232 14
3. Benettin et al. (1980) - Lyapunov exponents computation
4. Froeschlé et al. (1997) - FLI definition and applications
5. Cincotta & Simó (2000) - MEGNO method
6. Pesin (1977) - Entropy-formula connection
7. **Chaos and rotating black holes with halos**
   P.S. Letelier (Campinas State U., IMECC), W.M. Vieira (Campinas State U., IMECC), Phys.Rev.D 56 (1997), 8095-8098
8. **Stability of Orbits around a Spinning Body in a Pseudo-Newtonian Hill Problem**
   A.F. Steklain (Campinas State U., IMECC), P.S. Letelier (Campinas State U., IMECC), Phys.Lett.A 373 (2009), 188-194
9. **Influence of the black hole spin on the chaotic particle dynamics within a dipolar halo**
   Sankhasubhra Nag, Siddhartha Sinha, Deepika B. Ananda, Tapas K Das, Astrophys.Space Sci. 362 (2017) 4, 81
10. **Stealth Chaos due to Frame Dragging**
    Andrés F. Gutiérrez-Ruiz, Alejandro Cárdenas-Avendaño, Nicolás Yunes, Leonardo A. Pachón,abff99 (publication)

Quantitative synthesis: global chaos trends via θ

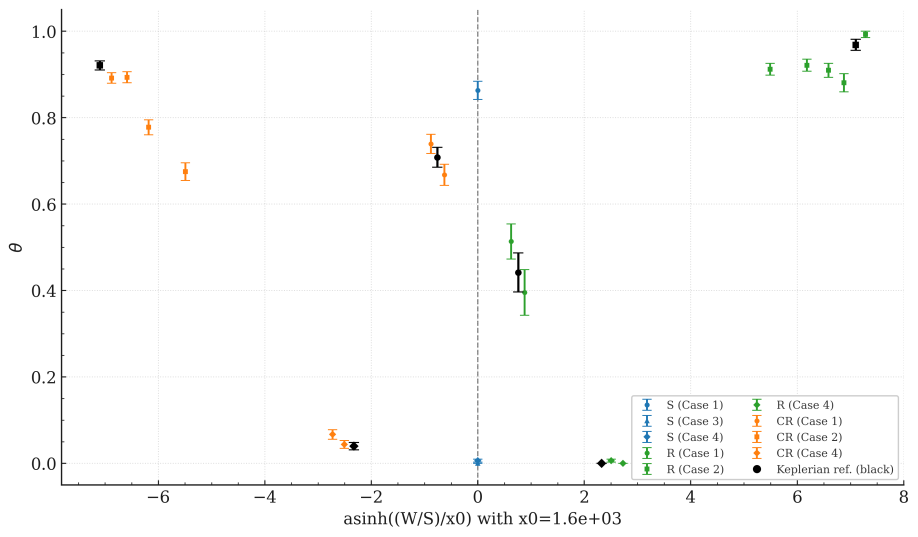

Example application Gaussian Mixture Model (GMM)

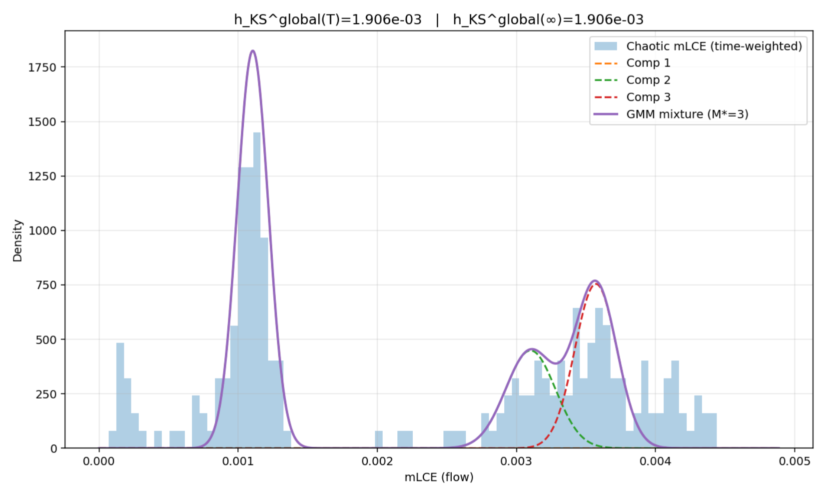

Figure: Enter Caption

Quantity	Value			
Total orbits N_{tot}	263			
Chaotic orbits N_{cha} (MEGNO ≥ 6.0)	227			
Chaotic time fraction θ	0.863119			
Selected components M^* (GMM)	2			
$h_{KS}^{global}(T)$	1.972058×10^{-3}			
$h_{KS}^{global}(\infty)$	1.972058×10^{-3}			
Components (GMM)				
layer	μ_m	c_{cond}	c_{glob}	σ_m
1	3.503619×10^{-3}	0.5165	0.4458	4.921810×10^{-4}
2	9.829661×10^{-4}	0.4835	0.4173	3.015106×10^{-4}
REG	0.000000×10^{0}	0.0000	0.1369	–

Table: Summary of the KS entropy calculation for $S1$

Estimating GMM Peaks and Their Uncertainty

1. **Data and selection.** For each orbit i, we label it chaotic using the strict MEGNO gate ($Y \geq 6$). Let $N_{\rm tot}$ be the number of sampled orbits, $N_{\rm cha}$ the chaotic subset size, and $\theta = N_{\rm cha}/N_{\rm tot}$ the global chaotic fraction. From chaotic orbits we collect one positive rate per orbit (e.g. local Lyapunov estimate), denoted $\lambda_i(T)$.
2. **Model (1D GMM).** We fit a Gaussian Mixture Model (EM algorithm) to $\{\lambda_i(T)\}_{\text{cha}}$ with candidate component counts $M = 1, \ldots, M_{\text{max}}$ and select M^* by BIC. We use diagonal covariances with a small regularization to avoid degeneracy and reject spurious tiny components via a minimum weight floor.
3. **Peaks ("layers").** Each component m has mean μ_m, standard deviation σ_m, and chaotic-set weight p_m ($\sum_m p_m = 1$). We report:

$$c_{{\rm cond},m} = p_m, \qquad c_{{\rm glob},m} = \theta\, p_m.$$

   For well-separated components, the peak location is μ_m. (We require $|\mu_m - \mu_{m'}| \gtrsim 2(\sigma_m + \sigma_{m'})$ to call peaks distinct; otherwise we interpret them as a single broad peak.)

4. **Global KS-entropy (at time T).**

$$h_{KS}^{\mathrm{global}}(T) = \sum_{m=1}^{M^*} \mu_m \, c_{\mathrm{glob},m} = \theta \sum_{m=1}^{M^*} p_m \mu_m,$$

since regular orbits contribute zero.

5. **Uncertainty.** The effective sample in component m is $N_m = N_{\mathrm{cha}}\, p_m$. The (asymptotic) standard error of the peak position is

$$\sigma_{\mathrm{tot}}(\mu_m) \;=\; \frac{\sigma_m}{\sqrt{N_m}} \;=\; \frac{\sigma_m}{\sqrt{N_{\mathrm{cha}}\, p_m}}.$$

A conservative first-order error for $h_{KS}^{\mathrm{global}}(T)$ (ignoring covariances) is

$$\sigma_{\mathrm{tot}}^2\left[h_{KS}^{\mathrm{global}}\right] \approx \sum_m c_{\mathrm{glob},m}^2 \, \mathrm{SE}(\mu_m)^2 \;+\; \theta^2 \sum_m \mu_m^2 \, \frac{p_m(1-p_m)}{N_{\mathrm{cha}}} \;+\; \Big(\sum_m \mu_m p_m\Big)^2 \frac{\theta(1-\theta)}{N_{\mathrm{tot}}}.$$

When $N_{\mathrm{cha}} = 0$, no GMM is fitted, $\lambda_+ = 0$, and $h_{KS} = 0$.

FLI evolution in S1 (log–log view)

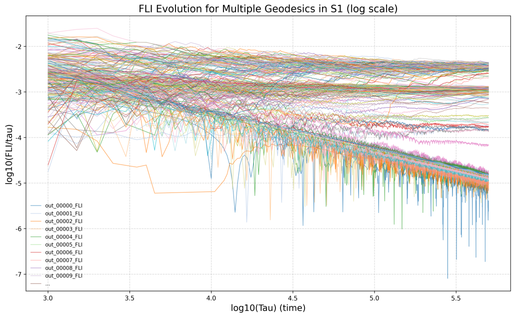

- Each curve: one geodesic; ordinate is $\log_{10}(\mathrm{FLI}/\tau)$ vs. $\log_{10}\tau$.
- Regular motion: after transients, trajectories follow near power–law decay (approximately straight lines with negative slope).
- Chaotic candidates: curves deviating upward or flattening (relative growth of FLI), often separating from the bulk.
- Use: fast, population–level screening of divergence rates and early outlier detection.

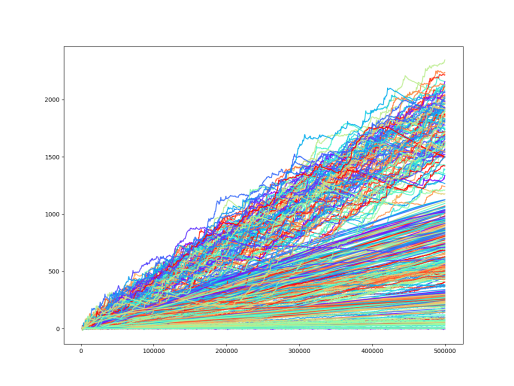

- Simultaneous time–evolution of FLI and MEGNO for many orbits.
- Regular: MEGNO saturates near $\langle Y \rangle \approx 2$ and FLI grows slowly.
- Chaotic: MEGNO grows approximately linearly with time and FLI rises rapidly.
- Use: cross–validation of classifications and identification of time windows where diagnostics agree.

FLI evolution (linear scale)

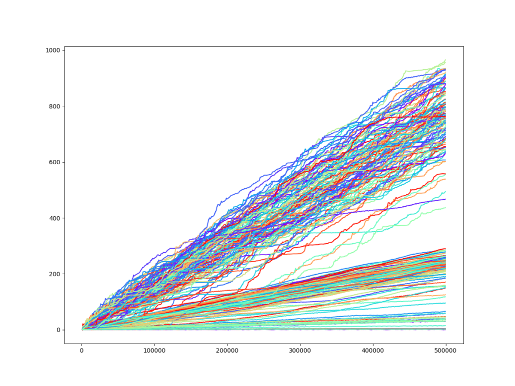

- Same ensemble as Slide 2 but with linear ordinate for FLI.
- Highlights separation between slowly growing (regular) and rapidly growing (chaotic) trajectories.
- Useful to inspect transients, saturation, and the spread of growth rates without logarithmic compression.

mLCE distribution (violin plot)

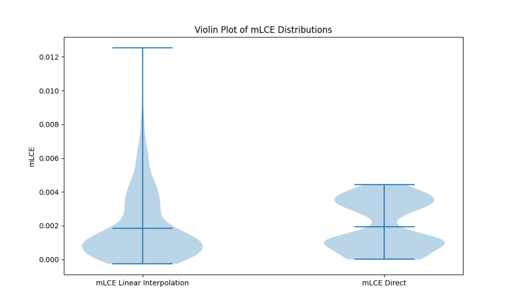

- Violin plots compare the distributions of estimated maximal Lyapunov exponents (mLCE) from two estimators.
- Center lines indicate medians; the thickness encodes the probability density (spread).
- Interpretation: differences in median and spread reflect estimator bias and variance; narrow violins imply more stable estimates.
- Use: choose the estimator and quantify distributional uncertainty across the orbit sample.

Definition of chaos

Khaos

The word *khaos* coming from Ancient Greek mythology and literally means "gap, abyss"referring to the primeval emptiness of the universe before things came into being or the abyss of Tartarus, the underworld.

Definition of chaos

Khaos

The word *khaos* coming from Ancient Greek mythology and literally means "gap, abyss"referring to the primeval emptiness of the universe before things came into being or the abyss of Tartarus, the underworld.

Chaos Theory

It is a mathematical field of study whose main aim is to study of the non-linear dynamics of complex systems whose behaviour at first sight seems to be random and not predictable, chaotic, but it is indeed deterministic.

Definition of chaos

Khaos

The word *khaos* coming from Ancient Greek mythology and literally means "gap, abyss"referring to the primeval emptiness of the universe before things came into being or the abyss of Tartarus, the underworld.

Chaos Theory

It is a mathematical field of study whose main aim is to study of the non-linear dynamics of complex systems whose behaviour at first sight seems to be random and not predictable, chaotic, but it is indeed deterministic.

1. long-term predictions are in general impossible for this systems
2. **sensitive dependence on initial conditions**

Definition of chaos

Khaos

The word *khaos* coming from Ancient Greek mythology and literally means "gap, abyss"referring to the primeval emptiness of the universe before things came into being or the abyss of Tartarus, the underworld.

Chaos Theory

It is a mathematical field of study whose main aim is to study of the non-linear dynamics of complex systems whose behaviour at first sight seems to be random and not predictable, chaotic, but it is indeed deterministic.

1. long-term predictions are in general impossible for this systems
2. **sensitive dependence on initial conditions**

"...a butterfly flapping its wings in Brazil can produce a tornado in Texas."
Edward Norton Lorenz *(meteorologist)*

Let $(M, H(\bar{p}, \bar{q}))$ be a nd Hamiltonian system for which exists a set of n functions, f_i which are first integrals of the motion and are in involution :$\{f_i, f_j\} = 0$, $\forall i, j$
If the manifold defined by the level sets of these functions is compact and connected

$$M_c = \{(\bar{p}, \bar{q}) : f_i(\bar{p}, \bar{q}) = c_i\}, \qquad c_i \in R$$

it is diffeomorphic to a n torus ($T^n = S^1 x \ldots x S^1$ n times) and it is possible to perform a canonical transformation in action-angle coordinates

$$(\bar{p}, \bar{q}) \quad \longrightarrow \quad (\bar{I}, \bar{\theta}) \in R^n x T^n \qquad \Rightarrow \qquad H(\bar{I}, \bar{\theta}) = h(\bar{I}) \tag{1}$$

where the motion of the angle-variables is linear and the frequencies fixed.

$$\bar{I} = I_0 = const \qquad \bar{\theta} = \bar{\theta}_0 + \omega(\bar{I}_0)t. \tag{2}$$

The system is then integrable by quadrature and the phase-space will results foliated in invariant tori each corresponding to a given set of frequencies.

Resonances

Let it be det $\left|\partial\bar{\omega}/\partial\bar{I}\right| \neq 0$ (non-degenerate system), then there if the frequencies satisfy a relation of the following type

Resonant condition

$$\sum_{i=1}^{n} k_i\omega_i = 0$$

$k_i \in Z, \qquad |k| = \sum_{i=1}^{n} |k_i| \neq 0$

Depending on the number of such relations, m, there can be different consequences:

1. $m = 0$ "Irrational ratio between frequencies": The motion is on $T^{(n)}$ and it is "quasi-periodic", that is the orbit fill the tori densely but they never close.
2. $0 < m < n - 1$ "Not all frequencies are linear independent": The motion is on $T^{(n-m)}$ and it is "quasi-periodic" on them, that is the orbit fill the tori densely but they never close.
3. $m = n - 1$ "All frequencies are proportional": The motion is on T and it is "periodic", that is the orbit close.

A non-degenerate, integrable system with n degrees of freedom, when slightly perturbed

$$H(\bar{\theta}, \bar{I}) = h(\bar{I}) + \epsilon H_1(\bar{\theta}, \bar{I})$$

must satisfy the **diophantic condition**

$$\Big|\sum_{i=1}^{n} \omega_i k_i\Big| > \frac{O(\epsilon)}{\left(\sum_{i=1}^{n} |k_i|\right)^d}, \qquad k_i \in N, d > (n-1)$$

The motion still occur on tori, but they are deformed (KAM non-resonant tori), while far away from the resonances, the phase-space appears very similar to the correspondent unperturbed motion

(1912) Last geometric theorem of Poincaré

Poincaré-Birkoff Theorem

When an integrable system is perturbed, the resonant tori are destroyed and only a finite even number of fixed points of a given period survive. Half of them will be stable points, the other half unstable points.

When an integrable system is perturbed, the resonant tori are destroyed and only a finite even number of fixed points of a given period survive. Half of them will be stable points, the other half unstable points.

Consequences $\Rightarrow$ **Birkhoff chains**

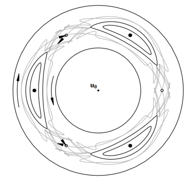

1. **island of stability**: They are set of resonant KAM curves around stable points, characterized by particular value of the frequencies ratio (**regular orbits**).
2. **Irregular orbits** emanates from the asymptotic manifolds of unstable points following complicated path and filling the chaotic layers.